NIH Public Access
Author Manuscript
Mol Cancer Ther. Author manuscript; available in PMC 2012 May 09.

Published in final edited form as:
Mol Cancer Ther. 2009 May ; 8(5): 1378–1386. doi:10.1158/1535-7163.MCT-08-1170.

Targeting the cancer stroma with a fibroblast activation protein-activated promelittin protoxin

Aaron M. LeBeau[1], **W. Nathaniel Brennen**[1], **Saurabh Aggarwal**[2], and **Samuel R. Denmeade**[1,2,3]

[1]Department of Pharmacology and Molecular Sciences, Johns Hopkins The Johns Hopkins University, Baltimore Maryland [2]Department of Chemical and Biomolecular Engineering, Johns Hopkins The Johns Hopkins University, Baltimore Maryland [3]The Sidney Kimmel Comprehensive Cancer Center, Johns Hopkins The Johns Hopkins University, Baltimore Maryland

Abstract

Fibroblast-Activation Protein-α (FAP) is a membrane-bound serine protease that is expressed on the surface of reactive stromal fibroblasts present within the majority of human epithelial tumors but is not expressed by normal tissues. FAP is a postprolyl peptidase that differs from other dipeptidyl prolyl peptidases such as di-prolylpeptidase 4 in that it also has gelatinase and collagenase endopeptidase activity. Therefore, FAP represents a potential pan-tumor target whose enzymatic activity can be exploited for the intratumoral activation of prodrugs and protoxins. To evaluate FAP as a tumor-specific target, putative FAP-selective peptide protoxins were constructed through modification of the prodomain of melittin, a 26 amino acid amphipathic cytolytic peptide that is the main toxic component in the venom of the common European honeybee *Apis milefera*. Melittin is synthesized as promelittin, containing a 22 amino acid NH_2-terminal prodomain rich in the amino acids proline and alanine. In this study, peptides containing truncated melittin prodomain sequences were tested on erythrocytes to determine the optimal prodomain length for inhibiting cytolytic activity. Once optimized, modified promelittin peptides were generated in which previously identified FAP substrate sequences were introduced into the prodomain. Peptide protoxins were identified that were efficiently activated by FAP and selectively toxic to FAP-expressing cell lines with an IC_{50} value in the low micromolar range that is similar to melittin. Intratumoral injection of an FAP-activated protoxin produced significant lysis and growth inhibition of human breast and prostate cancer xenografts with minimal toxicity to the host animal.

Introduction

The growth of an epithelial neoplasm requires the formation of a supporting tumor stroma to supply nutrients and growth factors for tumor cell survival and continued growth. This invasive growth is associated with characteristic changes in the supporting stroma that include the induction of tumor blood vessel formation; the recruitment of reactive stromal fibroblasts, lymphocytes, and macrophages; the release of peptide-signaling molecules and proteases; and the production of an altered extracellular matrix (1–5). The tumor stroma

Copyright © 2009 American Association for Cancer Research.

Requests for reprints: Samuel R. Denmeade, Department of Oncology, The Johns Hopkins University School of Medicine, Cancer Research Building I, Rm 1M43, 1650 Orleans Street, Baltimore, MD 21231. Phone: 410-955-8875; Fax: 410-614-8397. denmesa@jhmi.edu.

Disclosure of Potential Conflicts of Interest
No potential conflicts of interest were disclosed.

NIH-PA Author Manuscript
NIH-PA Author Manuscript
NIH-PA Author Manuscript
Johns Hopkins University EX2036
GE Healthcare v. Johns Hopkins
PGR2025-00059

NIH-PA Author Manuscript

NIH-PA Author Manuscript

NIH-PA Author Manuscript

compartment represents a major component of the mass of most carcinomas, with 20% to 50% commonly seen in breast, lung, and colorectal cancers and reaching >90% in carcinomas that have desmoplastic reactions (5, 6).

Reactive tumor stromal fibroblasts differ from fibroblasts of normal adult tissues with regard to morphology, gene expression profiles, and production of important biological mediators such as growth factors and proteases (1, 7, 8). A highly consistent trait of tumor stromal fibroblasts is the induction of the membrane-bound serine protease fibro-blast-activation protein-α (FAP). FAP was originally identified as an inducible antigen expressed on reactive stroma and given the name Fibroblast Activation Protein. FAP was independently identified by a second group as a gelatinase expressed by aggressive melanoma cell lines and was given the name “seprase” for surface expressed protease (9). Subsequent cloning of FAP and seprase revealed that they are the same cell-surface serine protease (10).

FAP was originally reported to be a cell-surface antigen recognized by the F19 monoclonal antibody on human astrocytes and sarcoma cell lines *in vitro* (11). In one series using human tissues, FAP was detected in the stroma of over 90% of malignant breast, colorectal, skin, and pancreatic tumors (7, 11). In a small study, FAP was detected in the stroma of 7of 7 prostate cancers (12). FAP is also expressed by a subset of soft tissue and bone sarcomas (7). FAP-positive fibroblasts also accompany newly formed tumor blood vessels (10). In nonmalignant tissue, FAP is expressed by reactive fibroblasts in wound healing, rheumatoid arthritis, liver cirrhosis, and in some fetal mesenchymal tissues (7). Cheng et al. (13) also showed that, such as human FAP, mouse FAP is expressed by reactive fibroblasts within human cancer xenografts. In contrast, most normal adult tissues show no detectable FAP protein expression (7). In a recent study, Ghilardi et al. (14) used real-time PCR to quantify gene expression from laser capture dissected tumor endothelium and found a significant increase in FAP expression compared with normal endothelium. This suggests that FAP expression may also be induced in both reactive tumor stroma and endothelium.

FAP is a member of the enzyme class known as postprolyl peptidases that are uniquely capable of cleaving the Pro-Xxx amino acid bond (15). This group of proteases includes the well-characterized dipeptidyl peptidase 4 (DPP4) as well as DPP2, DPP6, DPP7, DPP8, DPP9, prolyl carboxypeptidase, and prolyl endopeptidase. The substrate preferences for many of these prolyl peptidases are not entirely known but, such as DPP4, they all have dipeptidase activity. Like DPP4, FAP is a type II integral membrane protein able to cleave peptides containing proline as the penultimate amino acid. FAP differs from DPP4 in that it also has gelatinase and collagenase activity (16). This additional gelatinase/collagenase activity may be unique to FAP among the family of prolyl proteases.

The selective tumor expression and unique enzymatic activity of FAP make it a potentially attractive therapeutic target. Recently, our laboratory mapped all of the FAP cleavage sites in recombinant human gelatin and identified a series of peptide substrates that are efficiently cleaved by FAP (17). These peptide substrates can be coupled to cytotoxic small molecules to make FAP-activated prodrugs. Alternatively, the peptides could be incorporated into the activation domain of cytolytic proteins and peptides to produce FAP-activated protoxins. In this regard, we have generated an FAP-activated peptide toxin by incorporating an FAP-selective peptide sequence into the prodomain of the cytolytic peptide melittin.

Melittin, a 26 amino acid amphipathic peptide, is the main toxic component in the venom of the common European honeybee *Apis milefera* (18). The ability of melittin to induce the lysis of prokaryotic and eukaryotic cells has been well-documented (19–21). The exact mechanism by which melittin disrupts both natural and synthetic phospholipid bilayers is still largely unknown. In an aqueous milieu, melittin has a net + 6 charge and exists as a

NIH-PA Author Manuscript

NIH-PA Author Manuscript

NIH-PA Author Manuscript

random coiled monomer. It has been suggested that melittin can produce its toxic effects either by forming a transmembrane pore structure made up of melittin aggregates or by binding to the membrane surface and acting in a detergent-like manner leading to an increase in membrane permeability (18, 21).

In the honeybee, melittin is secreted into the venom glands as promelittin possessing an NH_2-terminal prodomain made up of 22 amino acids. The prodomain is highly negatively charged containing nine acidic amino acid residues (22). The presence of the prodomain confers an overall negative charge to the molecule and decreases the ability of melittin to interact with the surface of the cell membrane. In the prodomain amino acid sequence, every second amino acid is either proline or alanine. Promelittin activation *in vivo* is the result of the stepwise cleavage of the prodomain into 11 dipeptide fragments by a DPP4-like protease present in honeybee venom gland extracts (22). By acetylating the promelittin peptide or adding an extra amino acid residue at the NH_2 terminus, the stepwise activation of promelittin by DPP4 dipeptidase activity is prevented. This observation suggested that the promelittin prodomain could be readily reengineered to produce a prodomain that can be removed by a non–DPP4-like endopeptidase such as FAP. In this study, we report studies done to determine the minimal prodomain length required to inactivate the cytolytic activity of melittin. Subsequently, we substituted putative FAP peptide substrates into this truncated prodomain to identify an FAP-melittin peptide that is selectively toxic to FAP-producing cells. Finally, we evaluated the anti-tumor effect of an FAP-melittin protoxin after intratumoral injection of peptide into human prostate and breast cancer xenografts.

Materials and Methods

All reagents for Fmoc solid-phase peptide synthesis were purchased from Anaspec. Unless stated otherwise, all other reagents were purchased from Sigma. His-tagged FAP lacking the transmembrane domain was produced and purified in our laboratory as previously described (17). FAP activity was confirmed through activation of the dipeptide substrate Ala-Pro-AFC.

Cell Lines

The human prostate cancer cell line LNCaP and the human breast cancer cell line MCF-7 were purchased from American Type Culture Collection. LNCaP was maintained in RPMI 1640 and MCF-7 in DMEM media supplemented with 10% serum, 1% pen/strep, and 2 mmol/L L-glutamine (Invitrogen) in a 37°C incubator with 5% CO_2 and 98% humidity as previously described (23).

Generation of FAP-Transfected Cells

The full-length human FAP cDNA was generated as previously described (17) and cloned into the multiple cloning site of a pIRESneo3 vector (Clontech). Neomycin-selected colonies were obtained and evaluated for FAP expression through fluorescence-activated cell sorting analysis using supernatant from an anti-FAP F19 monoclonal antibody producing hybridoma line obtained from American Type Culture Collection as the primary antibody. Colonies expressing the highest levels of FAP were expanded and maintained under neomycin selection for use in *in vitro* studies.

Peptide Synthesis

Promelittin peptides were synthesized on Fmoc-Gln(Trt) Rink amide 4-methyl benzhydrylamine resin and were elongated using standard Fmoc solid-phase peptide conditions on an AAPPTEC Apex 396 peptide synthesizer as previously described (24). The prodomain for each peptide was of variable length, but the mature melittin peptide sequence,

NIH-PA Author Manuscript

NIH-PA Author Manuscript

NIH-PA Author Manuscript

NH_2-GIGAVLKVLTTGLPALISWIKRKRQQ-NH_2, was the same for each peptide. The cleavage and deprotection of the peptides from the resin were carried out using a cleavage cocktail of trifluoroacetic acid/thioanisole/water/phenol/EDT (82.5:5:5:5:2.5, v/v) for 4 h. The peptides were precipitated from the cleavage cocktail using cold ether and dissolved in water for reversed-phase high-performance liquid chromatography purification. Reversed-phase high-performance liquid chromatography purification was done on a Waters Δ 600 semiprep system using a Phenomenex Luna 10u C_{18} 250 × 10 mm semiprep column. The high-performance liquid chromatography gradient profile was linear starting at 100% solvent A (0.1% tri-fluoroacetic acid in H_2O) and changing to 100% solvent B (0.1% trifluoroacetic acid in acetonitrile) over 25 min with a flow rate of 8 mL/min. Fractions of the desired purity (>95% as determined using an analytic reversed-phase high-performance liquid chromatography) were pooled and lyophilized. The purified promelittin peptides were mass analyzed on an Applied Biosystems Voyager DE-STR MALDI-TOF mass spectrometer at the Johns Hopkins School of Medicine Mass Spectrometry and Proteomics Facility using a matrix of 10 mg/mL 2,5-dihydroxy benzoic acid in 50% ethanol/water. The mass spectrometer was calibrated using the ProteoMass Peptide MALDI Calbration kit (Sigma). All spectra were acquired in the positive ion mode.

Hemolysis Assays

Hemolysis assays were done as previously described (23). Briefly, peptides were dissolved in DMSO and serially titrated by 2-fold dilution using 1× PBS buffer. The peptides were incubated over a range of concentrations with washed human RBC at a concentration of 2% v/v for 1 h at 37°C. The control for zero hemolysis was RBCs suspended in PBS buffer alone, and the 100% hemolysis control consisted of RBCs in the presence of 1% Triton X-100. After incubation with the peptides, the RBCs were pelleted and 50 μL of each sample were transferred in triplicate to a clear flat-bottomed 96-well polystyrene plate. Hemolysis was assessed by measuring the absorbance of the samples at 540 nm with a Molecular Devices Spectra Max Plus automatic plate reader.

Promelittin FAP Digestion

One hundred micrograms of each promelittin peptide were incubated with 2 μg of purified FAP in 200 μL of FAP assay buffer containing 100 mmol/L Tris, 100 mmol/L NaCl (pH 7.8) at 37°C. Aliquots of the digests were taken every hour for 8 h, desalted using P10-C_{18} ZipTips (Millipore), and spotted (0.5 μL) on a MALDI-TOF plate using the 2,5-dihydroxy benzoic acid matrix. Spectra were collected on an Applied Biosystems Voyager DE-STR MALDI-TOF mass spectrometer in positive ion mode.

Cytotoxicity Assays

Assays were done using MCF-7 breast cancer cells transfected with a full-length FAP expression vector. Vector only–transfected MCF-7 cells served as a control. Cells were exposed to peptides over a range of concentrations for 72 h prior and then cell viability was determined using an 3-(4,5-dimethylthiazol-2-yl)-2,5-diphenyltetrazolium bromide cell proliferation assay (Promega) as previously described and according to manufacturer's instructions (23).

In vivo Assays: Tumor Xenograft Studies

Mouse care and treatment was approved by and done in accordance with the guidelines of the Animal Care and Use Committee of the Johns Hopkins University School of Medicine. Cells maintained under standard conditions were detached by treatment with 0.25% trypsin-EDTA solution and washed in HBSS. They were then suspended in a 60% mixture of Matrigel Matrix (BD Biosciences) in HBSS at a concentration of 2.0×10^6 cells per 100 μL

NIH-PA Author Manuscript

NIH-PA Author Manuscript

NIH-PA Author Manuscript

of solution. LNCaP cells were then injected into the subcutis overlying the rear flanks of 6-week-old male nude mice (Harlan). MCF-7 cells were injected s.c. into 6-wk-old female nude mice previously implanted s.c. with a slow release estrogen pellet (0.72 mg of 17β-estradiol; Innovative Research of America) in the contralateral flank. Weekly tumor measurements were made with calipers and the tumor volume (in cm^3) was calculated by the formula $0.5236 \times L \times W \times H$. The mice were euthanized by CO_2 overdose, and the tumors were weighed and processed for histochemical analysis as previously described (23). Balb-c mice (Harlan) were used for i.v. toxicity studies as previously described (23).

Statistical Analysis

For the *in vitro* proliferation studies, *P* values were derived from the Student's *t* test. All statistical tests were two-sided, and *P* value of <0.05 was considered to be statistically significant. For the *in vivo* studies, data, presented as mean ± SE, were evaluated using ANOVA analysis. *P* value of <0.05 was considered statistically significant.

Results

Promelittin Prodomain Truncation

A total of 22 promelittin peptides, representing every possible prodomain length, were synthesized (Table 1). Using the truncated promelittin peptides, we investigated how much of the prodomain was necessary to inhibit the cytolytic ability of melittin. The goal was to find the minimal length melittin prodomain that could be subsequently modified to produce the minimal length FAP-activated melittin peptide toxin. Whereas PM11 represents the full-length prodomain, peptides PM0-PM10 represent products of the stepwise two amino acid cleavage of promelittin by DPP4. Peptides PM1a-PM11a are non-DPP4 substrates because they do not contain dipeptide units at the NH_2 terminus ending with either proline or alanine. To assess the relative degree of inhibition of the lytic ability of each promelittin peptide toward eukaryotic cells, human erythrocytes were used as a model membrane. The hemolytic dose necessary to lyse 50% of the erythrocytes (i.e., HD_{50}) was determined for each promelittin peptide (Table 1). These studies revealed that the promelittin peptides containing the longest prodomains were the least hemolytic toward human erythrocytes. The full-length promelittin peptide (PM11), PM11a, PM10, and PM10a, all had HD_{50} values above 100 μmol/L. Appreciable hemolysis was not observed until approximately half of the prodomain had been removed. PM6, with a 12 amino acid prodomain sequence and a net charge of 0, had an HD_{50} of 55.9 μmol/L. As the prodomain sequence decreased one amino acid at a time and the net negative charge of the peptide increased, the HD_{50} for each peptide steadily decreased (Table 1). PM0 (melittin) was found to have an HD_{50} of 1.3 μmol/L. Likewise, the 7 shortest promelittin peptides were hemolytic with HD_{50} values at or below 10 μmol/L.

Based on these results, the 14 amino acid prodomain length of PM7, which had an HD_{50} of 66.6 μmol/L, was selected for further studies aimed at developing an FAP-activated toxin. PM7 was found to be ~50-fold less hemolytic than the fully processed melittin. Although longer length prodomains had higher HD_{50} values in the hemolysis assay, the 40 amino acid PM7 was selected because this starting peptide length allowed for the introduction of modifications and additions to the prodomain that would produce peptides that were <50 amino acids in length. Peptides longer than 50 amino acids were technically difficult to synthesize and this precluded the use of longer length promelittins (e.g., PM11) as the starting sequence.

NIH-PA Author Manuscript

NIH-PA Author Manuscript

NIH-PA Author Manuscript

Generation of an FAP-Cleavable Promelittin Protoxins

Previous studies in our laboratory and others have documented that the most preferred FAP-cleavable peptide sequences contain Pro in the P1 position and Gly in the P2 position with a suggestion that Ala in the P′1 position is also favored (17, 25). Based on our previous studies characterizing FAP cleavage substrates from a map of cleavage sites within human gelatin, five candidate protoxins were synthesized using the prodomain of PM7 (i.e., FAP1-5; Fig. 1A; ref. 16). In FAP1, the Asp-4 of the PM7 prodomain was changed to a Gly to reproduce the Gly-Pro preference in the P1 and P2 positions ascribed to FAP (17). Because the effect on the ability of FAP to hydrolyze a peptide containing an acidic Glu residue in the P1 position was not known, FAP2 was designed such that the prodomain sequence was kept the same as that for FAP1 with the exception that Glu-2 of the prodomain of FAP1 was removed to create the FAP preferred P2-P1-P′1 sequence of Gly-Pro-Ala. For FAP3, the P2-P1-P′1 sequence of Gly-Pro-Ala was inserted between the NH_2 terminus of melittin and the full-length native PM7 prodomain sequence. FAP4 had a seven amino acid FAP cleavable peptide substrate (SGEAGPA) inserted between the NH_2 terminus and the PM7 prodomain, whereas FAP5 had a repetitive $(Pro\text{-}Gly\text{-}Pro)_2$ motif inserted between the NH_2 terminus of melittin and the prodomain of PM7. FAP4 and FAP5 were the two largest peptides synthesized, 46 and 47 amino acids, respectively. FAP2 was the shortest, consisting of only 39 amino acids. The hemolytic activity of these FAP candidate protoxins was assayed and all were found to have HD_{50} values between 50 and 70 μmol/L (Table 2).

FAP Cleavage Assays

To assess FAP cleavage, the FAP candidate protoxins were assayed *in vitro* with purified recombinant FAP to characterize the extent of FAP-mediated cleavage. The peptides (100 μg) were digested with FAP (2 μg) for a total of 8 hours at 37°C. Every 2 hours, aliquots were taken and the progress of the digest was monitored using matrix-assisted laser desorption/ionization time-of-flight (MALDI-TOF) mass spectrometry (Fig. 1). After 8 hours, the only protoxin that was completely digested by FAP was FAP2 (Fig. 1). The digested FAP2 yielded only 1 cleavage product with a mass of 2,918.32 m/z, corresponding to the hydrolysis of the Gly-Pro↓Ala bond. FAP1, which differed from FAP2 by only one Glu residue, did show some of the desired cleavage product at 3,046.89 m/z (Fig. 1). However, the FAP1 digest was incomplete, leaving uncut starting material and other cleavage by-products. FAP3, FAP4, and FAP5 were cleaved to varying degrees, but none were cleaved as well as FAP2 (Fig. 1). Finally, although mature melittin also contains an internal proline residue, MALDI-TOF analysis showed that it was not cleaved by FAP (data not shown).

FAP Promelittin Protoxins Selectively Kill FAP-Expressing Human Breast Cancer Cell Lines

To evaluate the selectivity of each FAP-activated protoxin for the ability to kill FAP-positive versus FAP-negative cancer cells, we transfected the human breast cancer cell line MCF-7 with either FAP or vector only controls. These cells were then used to assess the effect of each protoxin on growth as assayed by 3-(4,5-dimethylthiazol-2-yl)-2,5-diphenyltetrazolium bromide assay. In this assay, mature melittin showed no selectivity and was able to kill both cell lines at approximately equally low micromolar concentrations (Table 2). Compared with melittin, the modified promelittin peptides were ~30- to 40-fold less toxic against the vector only–transfected FAP-negative MCF-7 cells. In contrast, against the transfected FAP-producing cell line, FAP2 was the most toxic peptide surveyed with an IC_{50} of 5.2 μmol/L. This peptide was also the most selective and was ~7-fold more active against the FAP-positive versus FAP-negative MCF-7 cells. All of the other promelittin peptides had fold differences in cytotoxicity of less than two (Table 2). FAP2 was the only protoxin in this series that showed a significant therapeutic index *in vitro*.

NIH-PA Author Manuscript

NIH-PA Author Manuscript

NIH-PA Author Manuscript

To eliminate the potential for nonspecific cleavage of the FAP2 sequence by DPP4, we subsequently generated a DPP4-"resistant" version of FAP2 by adding an acetylated NH_2-terminal glycine to the FAP2 peptide to generate Ac-FAP6. Ac-FAP6 was cleaved by FAP to the same extent as FAP2 (data not shown) and had the highest HD_{50} (72 μmol/L) of all of the FAP-activated protoxins (Table 2). This acetylated peptide showed increased specificity with an IC_{50} of 47.9 versus 35.1 μmol/L for FAP2 against FAP-negative cells. However, Ac-FAP6 was nearly as potent as FAP2 with an IC_{50} value of 6.1 μmol/L against FAP-positive cells for an overall higher ~8-fold difference in toxicity against FAP-positive and FAP-negative cells.

In vivo Antitumor Activity of FAP Promelittin Protoxins

Before performing *in vivo* efficacy studies, we did toxicity studies *in vivo* with the administration of the protoxins i.v. and intratumorally. Melittin is a nonspecific cytolytic toxin. Therefore, as expected, melittin was highly toxic to mice with an i.v. LD_{100} (i.e., single dose that kills 100% of animals) of ~3 mg/kg. i.v., a dose of 1 mg/kg of melittin was the maximally tolerated dose. In contrast, for PM11, FAP2, and Ac-FAP6, a single dose of 40 mg/kg i.v. was tolerated in Balb-c mice, whereas a dose of 100 mg/kg was 100% lethal. The LD_{100} for FAP2 was subsequently found to be lower in tumor-bearing nude mice used in efficacy experiments as a single 40 mg/kg i.v. dose proved lethal to all mice within 1 week posttreatment. For the intratumoral injection studies, the maximum tolerated dose of intratumoral melittin was determined to be 5.7 mg/kg (50 nmoles). In contrast, an intratumoral dose of 40 mg/kg (250 nmoles) of FAP2 was well-tolerated, whereas a dose of 200 mg/kg (1,250 nmoles) was lethal to ~33% of treated animals by 24 hours posttreatment.

A number of studies have documented that FAP expression in mouse stromal cells occurs in a wide variety of human cancer xenografts (13, 26, 27). On the basis of these dose finding studies, an initial cohort of animals (n = 6 per group) bearing LNCaP human prostate cancer xenografts received a single intratumoral injection of either 40 or 200 mg/kg of FAP2 (Fig. 2). Tumors were then imaged serially over a 34-day period. Representative results are shown in Fig. 2. Treated tumors developed a necrotic center and overlying eschar, which eventually healed as the underlying tumor regressed over the observation period. Complete regressions were observed in select animals in the 200 mg/kg group (Fig. 2), but this dose level also resulted in the death of 1 of 3 of the treated animals. No complete regressions were observed in the 40 mg/kg dosing group.

The next experiment was designed to compare the extent of FAP specific versus nonspecific killing after the injection of a series of promelittin toxins into human MCF-7 breast cancer xenografts. This line was selected based on previous studies demonstrating that MCF-7 possesses a moderate amount of stroma and can induce expression of human FAP by human fibroblasts coinoculated with MCF-7 cells (28). For these studies, we compared the single dose efficacy of Ac-FAP6 (FAP-activated, DPP4-resistant, HD_{50} of 72 μmol/L) to PM11 (FAP-resistant, DPP4-activated, HD_{50} of >100 μmol/L). In addition, to generate a toxin that would not be cleaved by FAP or DPP4, we evaluated the effects of acetylating the amino terminus of the PM toxins. In this analysis, we determined that acetylation can lower the HD_{50} compared with the unacetylated protoxin in some instances. From this analysis, we selected the acetylated version of sequence PM9 for *in vivo* studies because this acetylated protoxin had the highest HD_{50} of all of the acetylated peptides tested. Although PM9 had an HD_{50} of 95 μmol/L, Ac-PM9 had an HD_{50} of 76 μmol/L, which was similar to the HD_{50} for Ac-FAP-6. Like Ac-FAP6, Ac-PM 9 is not a substrate for dipeptidyl peptidase IV due to acetylation of the amino terminus and is not cleaved by FAP due to lack of the FAP-preferred Gly-Pro dipeptide in the prodomain. Therefore Ac-PM9 can be considered FAP resistant and DPP4 resistant.

NIH-PA Author Manuscript

NIH-PA Author Manuscript

NIH-PA Author Manuscript

Based on previous toxicity studies, tumor-bearing animals were treated with a single intratumoral dose of 250 nmoles (~40–50 mg/kg) of each of these promelittin toxins. Tumors (n = 3 per group) were then harvested 96 hours postinjection, fixed, and stained. Areas of necrotic tissue were easily seen under low-power magnification with higher power magnification demonstrating areas with pyknotic nuclei in a field of cellular debris (Fig. 3A). Under low-power magnification using image analysis, the total area of the tumor slice was determined as previously described (23). Subsequently, the total area of nonviable tumor tissue was determined and the % area of necrosis was determined from the ratio of these two areas (Fig. 3B). Using this methodology, injection of PM11 resulted in tumors with ~25% necrosis of total tumor cross-sectional area, which was not significantly different than the 16% necrosis seen in control tumors injected with saline (Fig. 3C). Ac-PM9 induced necrosis that was not significantly different than that seen for PM11 (Fig. 3C). In contrast, Ac-FAP6 injection resulted in significant increase in the area of necrosis with ~60% necrosis of tumors at 96 hours postinjection, consistent with the enhanced distribution and activation of the Ac-FAP6 toxin compared with the non-FAP activated PM11 and Ac-PM9 toxins (Fig. 3C).

In the final experiment, the effect of Ac-FAP6 on the growth rate of tumors after intratumoral injection was compared with the growth rate of saline injected controls (Fig. 4A). Studies were done using an intratumoral treatment approach to evaluate the full extent of activation of the FAP-activated toxin within tumor tissue. After randomization to afford groups of relatively equal starting average tumor size, animals (n = 8 per group) received a single intratumoral injection of either 45 mg/kg (250 nmoles) of Ac-FAP6 or saline and were then followed for an additional 2 weeks posttreatment. No animal deaths or morbidity were observed in either group. In the saline controls, 7 of 8 animals had a doubling of tumor size by day 14 (Fig. 4B). In contrast, only 2 of 8 Ac-FAP6 animals had a doubling of tumor size over this time period (Fig. 4B). Two of the Ac-FAP6–treated animals had a >20% reduction in starting tumor size, with 1 of these animals having a >50% reduction. None of the control animals had any significant reduction in tumor size over the measurement period. A number of the Ac-FAP6 animals had an initial increase in tumor size at day 4 posttreatment followed by a 20% to 65% decrease in size at day 7 posttreatment, possibly due to an initial acute inflammation within the tumor.

Discussion

The goal of these studies was to show the feasibility of targeting the unique proteolytic activity of FAP, a membrane-bound serine protease that is expressed on the surface of reactive fibroblasts present within the stroma of most human tumors. Given its restricted expression in the reactive stroma of potentially >90% of epithelial cancers studied (7), FAP represents an attractive target for tumor-directed therapies. In this study, to provide the initial proof of concept data, we focused on a peptide-based protoxin strategy due to the ease of synthesis and the known ability of FAP to function as an endopeptidase. We showed that the inhibitory prodomain of melittin, a well-characterized toxin produced by the honeybee, could be modified to a form that was no longer hydrolyzed by the native activator protease DPP4 but, instead, was hydrolyzed by FAP.

Although FAP has only recently come to attention as a putative tumor-specific target, considerable effort has already been expended to develop FAP-based therapies. The most obvious therapeutic approach would be to develop inhibitors of FAP function such as monoclonal antibodies (29, 30) or small molecule inhibitors (31–33). These approaches are under preclinical and clinical evaluation. Such strategies would potentially produce a therapeutic benefit if FAP were involved in the promotion of growth within tumors. However, studies to date suggest that the role of FAP in tumor growth may be highly

NIH-PA Author Manuscript

NIH-PA Author Manuscript

NIH-PA Author Manuscript

contextual and in some cases, FAP expression may itself be growth inhibitory to tumors (33, 34). Thus, in contrast to these inhibitory strategies, the protoxin strategy described here can be successful regardless of the role of FAP in tumor biology as it takes advantage of the enzymatic activity of FAP to selectively activate a highly potent cytotoxin in the peritumoral fluid. Such activation should not only lead to death of tumor stromal cells but will also generate a significant bystander effect leading to death of tumor cells and endothelial cells within and surrounding the stromal compartment.

Although these studies provide proof of concept, the therapeutic application of this FAP-activated promelittin toxin is limited and would most likely only be useful in settings where intratumoral/intraorgan injection is possible. As an example of the applicability of such an approach, we described the development of a prostate-specific antigen–activated bacterial protoxin that is currently undergoing clinical testing as an intraprostatic therapy for the treatment of locally recurrent prostate cancer and benign prostatic hyperplasia (23). A similar strategy could be envisioned for the FAP-activated toxin. Because increased FAP expression has been found in most tumors evaluated, this approach could have a wider intratumoral application than that for a tissue-restricted protease such as prostate-specific antigen.

For these studies, we used an intratumoral treatment based approach to document that FAP-activated peptide toxin could produce a significant antitumor effect. Ideally, systemic delivery of these peptide toxins would be the preferred route administration. However, the ability of these promelittin toxins to induce hemolysis even when not fully processed represents a major hurdle to this application. In our hands, a single dose of 40 mg/kg of the FAP2 toxin, which was well-tolerated and effective intratumorally, proved lethal to tumor-bearing animals when administered i.v. This is most likely due to the fact that this dose would produce a potential maximum blood concentration that is >100 μmol/L, which is above the HD_{50} for this promelittin toxin. Further development of this promelittin peptide–based approach as a systemic therapy would require substantial modification to generate a protoxin that was unable to cause hemolysis even at millimolar concentrations. Alternatively, potent cytotoxic agents, preferably ones that did not produce hemolysis could be coupled to an FAP-specific peptide to generate an inactive prodrug that is selectively activated by FAP-expressing cells within the tumor stroma. Our laboratory has already adopted such an approach to generate prostate tissue specific prodrugs that are activated by the proteolytic activity of prostate-specific antigen, human glandular kallikrein 2, and prostate-specific membrane antigen (35–37). In ongoing studies in our laboratory, we are evaluating a series of such FAP-activated prodrugs that can be used to selectively target and kill cells within the tumor stroma as therapy for a wide variety of human cancers.

Acknowledgments

Grant support: NIH grant 5RO1CA124764 to SRD and a DOD prostate cancer predoctoral mentorship grant W81XWH-07 (W.N. Brennen).

We thank Marc Rosen for the excellent technical assistance in performing animal studies and the Johns Hopkins School of Medicine Mass Spectrometry and Proteomics Core Facility for assistance with the characterization of peptide toxins.

References

1. Dvorak HF. Tumors: wounds that do not heal. Similarities between tumor stroma generation and wound healing. N Engl J Med. 1986; 315:1650–9. [PubMed: 3537791]
2. Liotta LA, Steeg PS, Stetler-Stevenson WG. Cancer metastasis and angiogenesis: an imbalance of positive and negative regulation. Cell. 1991; 64:327–36. [PubMed: 1703045]

NIH-PA Author Manuscript
NIH-PA Author Manuscript
NIH-PA Author Manuscript

3. Basset P, Bellocq JP, Wolf C, et al. A novel metalloproteinase gene specifically expressed in stromal cells of breast carcinomas. Nature. 1990; 348:699–704. [PubMed: 1701851]
4. Brown LF, Guidi AJ, Schnitt SJ, et al. Vascular stroma formation in carcinoma *in situ*, invasive carcinoma, and metastatic carcinoma of the breast. Clin Cancer Res. 1999; 5:1041–56. [PubMed: 10353737]
5. Haslam SZ, Woodward TL. Host microenvironment in breast cancer development: epithelial-cell-stromal-cell interactions and steroid hormone action in normal and cancerous mammary gland. Breast Cancer Res. 2003; 5:208–15. [PubMed: 12817994]
6. Iozzo RV. Tumor stroma as a regulator of neoplastic behavior. Agonistic and antagonistic elements embedded in the same connective tissue. Lab Invest. 1995; 73:157–60. [PubMed: 7637316]
7. Garin-Chesa P, Old LJ, Rettig WJ. Cell surface glycoprotein of reactive stromal fibroblasts as a potential antibody target in human epithelial cancers. Proc Natl Acad Sci U S A. 1990; 87:7235–9. [PubMed: 2402505]
8. Aoyama A, Chen WT. A 170-kDa membrane-bound protease is associated with the expression of invasiveness by human malignant melanoma cells. Proc Natl Acad Sci U S A. 1990; 87:8296–300. [PubMed: 2172980]
9. Piñeiro-Sánchez ML, Goldstein LA, Dodt J, et al. Identification of the 170-kDa melanoma membrane-bound gelatinase (seprase) as a serine integral membrane protease. J Biol Chem. 1997; 272:7595–601. [PubMed: 9065413]
10. Scanlan MJ, Raj BK, Calvo B, et al. Molecular cloning of fibroblast activation protein α, a member of the serine protease family selectively expressed in stromal fibroblasts of epithelial cancers. Proc Natl Acad Sci U S A. 1994; 91:5657–61. [PubMed: 7911242]
11. Rettig WJ, Garin-Chesa P, Beresford HR, Oettgen HF, Melamed MR, Old LJ. Cell-surface glycoproteins of human sarcomas: differential expression in normal and malignant tissues and cultured cells. Proc Natl Acad Sci U S A. 1988; 85:3110–4. [PubMed: 2896356]
12. Tuxhorn JA, Ayala GE, Smith MJ, Smith VC, Dang TD, Rowley DR. Reactive stroma in human prostate cancer: induction of myofibroblast phenotype and extracellular matrix remodeling. Clin Cancer Res. 2002; 8:2912–23. [PubMed: 12231536]
13. Cheng JD, Dunbrack RL Jr, Valianou M, Rogatko A, Alpaugh RK, Weiner LM. Promotion of tumor growth by murine fibroblast activation protein, a serine protease, in an animal model. Cancer Res. 2002; 62:4767–72. [PubMed: 12183436]
14. Ghilardi C, Chiorino G, Dossi R, Nagy Z, Giavazzi R, Bani M. Identification of novel vascular markers through gene expression profiling of tumor-derived endothelium. BMC Genomics. 2008; 9:201. [PubMed: 18447899]
15. Kelly T. Fibroblast activation protein-α and dipeptidyl peptidase IV (CD26): cell-surface proteases that activate cell signaling and are potential targets for cancer therapy. Drug Resist Update. 2005; 8:51–8.
16. Park JE, Lenter MC, Zimmermann RN, Garin-Chesa P, Old LJ, Rettig WJ. Fibroblast activation protein, a dual specificity serine protease expressed in reactive human tumor stromal fibroblasts. J Biol Chem. 1999; 274:36505–12. [PubMed: 10593948]
17. Aggarwal S, Brennen WN, Kole TP, et al. Fibroblast activation protein peptide substrates identified from human collagen I derived gelatin cleavage sites. Biochemistry. 2008; 47:1076–86. [PubMed: 18095711]
18. Terwilliger TC, Eisenberg D. The structure of melittin. J Biol Chem. 1982; 257:6016–22. [PubMed: 7076662]
19. Unger T, Oren Z, Shai Y. The effect of cyclization on magainin 2 and melittin analogues on the structure, function, and model membranes interactions: implications to their mode of action. Biochemistry. 2001; 40:6388–97. [PubMed: 11371201]
20. Werkmeister JA, Hewish DR, Kirkpatrick A, Rivett DE. Sequence requirements for the activity of membrane active peptides. J Peptide Res. 2002; 60:232–8. [PubMed: 12366530]
21. Hristova K, Dempsey CE, White SH. Structure, location and lipid perturbations of melittin at the membrane interface. Biophysical J. 2001; 80:801–11.
22. Kreil G, Haiml L, Suchanek G. Stepwise cleavage of the pro part of promelittin by dipeptidylpeptidase 4. Eur J Biochem. 1980; 111:49–58. [PubMed: 7002560]

NIH-PA Author Manuscript

NIH-PA Author Manuscript

NIH-PA Author Manuscript

23. Williams SA, Merchant RF, Garrett-Mayer E, Isaacs JT, Buckley JT, Denmeade SR. A prostate-specific antigen-activated channel-forming toxin as therapy for prostatic disease. J Natl Cancer Inst. 2007; 99:376–85. [PubMed: 17341729]
24. Aggarwal S, Singh P, Topaloglu O, Isaacs JT, Denmeade SR. A dimeric peptide that binds selectively to prostate-specific membrane antigen and inhibits its enzymatic activity. Cancer Res. 2006; 66:9171–7. [PubMed: 16982760]
25. Edosada CY, Quan C, Wiesmann C, et al. Selective inhibition of fibroblast activation protein protease based on dipeptide substrate specificity. J Biol Chem. 2006; 281:7437–44. [PubMed: 16410248]
26. Ostermann E, Garin-Chesa P, Heider KH, et al. Effective immunoconjugate therapy in cancer models targeting a serine protease of tumor fibroblasts. Clin Cancer Res. 2008; 14:4584–92. [PubMed: 18628473]
27. Verel I, Heider KH, Siegmund M, et al. Tumor targeting properties of monoclonal antibodies with different affinity for target antigen CD44V6 in nude mice bearing head-and-neck cancer xenografts. Int J Cancer. 2002; 99:396–402. [PubMed: 11992408]
28. Tahtis K, Lee FT, Wheatley JM, et al. Expression and targeting of human fibroblast activation protein in a human skin/severe combined immunodeficient mouse breast cancer xenograft model. Mol Cancer Ther. 2003; 2:729–37. [PubMed: 12939462]
29. Scott AM, Wiseman G, Welt S, et al. A Phase I dose-escalation study of sibrotuzumab in patients with advanced or metastatic fibroblast activation protein-positive cancer. Clin Cancer Res. 2003; 9:1639–47. [PubMed: 12738716]
30. Hofheinz RD, al-Batran SE, Hartmann F, et al. Stromal antigen targeting by a humanised monoclonal antibody: an early phase II trial of sibrotuzumab in patients with metastatic colorectal cancer. Onkologie. 2003; 26:44–8. [PubMed: 12624517]
31. Adams S, Miller GT, Jesson MI, Watanabe T, Jones B, Wallner BP. PT-100, a small molecule dipeptidyl peptidase inhibitor, has potent antitumor effects and augments antibody-mediated cytotoxicity via a novel immune mechanism. Cancer Res. 2004; 64:5471–80. [PubMed: 15289357]
32. Aertgeerts K, Levin I, Shi L, et al. Structural and kinetic analysis of the substrate specificity of human fibroblast activation protein α. J Biol Chem. 2005; 280:19441–4. [PubMed: 15809306]
33. Wolf BB, Quan C, Tran T, Wiesmann C, Sutherlin D. On the edge of validation - cancer protease fibroblast activation protein. Mini-reviews in Med Chem. 2008; 8:719–727.
34. Ariga N, Sato E, Ohuchi N, Nagura H, Ohtani H. Stromal expression of fibroblast activation protein/seprase, a cell membrane serine proteinase and gelatinase, is associated with longer survival in patients with invasive ductal carcinoma of breast. Int J Cancer. 2001; 95:67–72. [PubMed: 11241314]
35. Denmeade SR, Jakobsen CM, Janssen S, et al. Prostate-specific antigen-activated thapsigargin prodrug as targeted therapy for prostate cancer. J Natl Cancer Inst. 2003; 95:990–1000. [PubMed: 12837835]
36. Janssen S, Rosen DM, Ricklis RM, et al. Pharmacokinetics, biodistribution, and antitumor efficacy of a human glandular kallikrein 2 (hK2)-activated thapsigargin prodrug. Prostate. 2006; 66:358–68. [PubMed: 16302271]
37. Mhaka A, Gady AM, Rosen DM, Lo KM, Gillies SD, Denmeade SR. Use of methotrexate-based peptide substrates to characterize the substrate specificity of prostate-specific membrane antigen (PSMA). Cancer Biol Ther. 2004; 3:551–8. [PubMed: 15044850]

NIH-PA Author Manuscript
NIH-PA Author Manuscript
NIH-PA Author Manuscript

	Prodomain Sequence	Observed Parental Ion (% Relative Intensity)	Observed Cleavage Product (% Relative Intensity)
FAP1	EP|EAEADAEAGP|EA -mel (3986.75 / 3046.89)	4214.71 (20)	3968.75 (30), 3046.89 (100)
FAP2	EPEAEADAEAGP|A -mel (2918.32)	4084.66 (0)	2918.32 (100)
FAP3	EPEAEADAEADPEAGP|A -mel (2918.48)	4497.73 (100)	2918.48 (70)
FAP4	EPEAEADAEADPEASGEAGP|A -mel (2918.93)	4841.82 (100)	2918.93 (30)
FAP5	EPEAEADAEADPEAPGPPGP|-mel (2846.13)	4774.14 (100)	2846.13 (15)

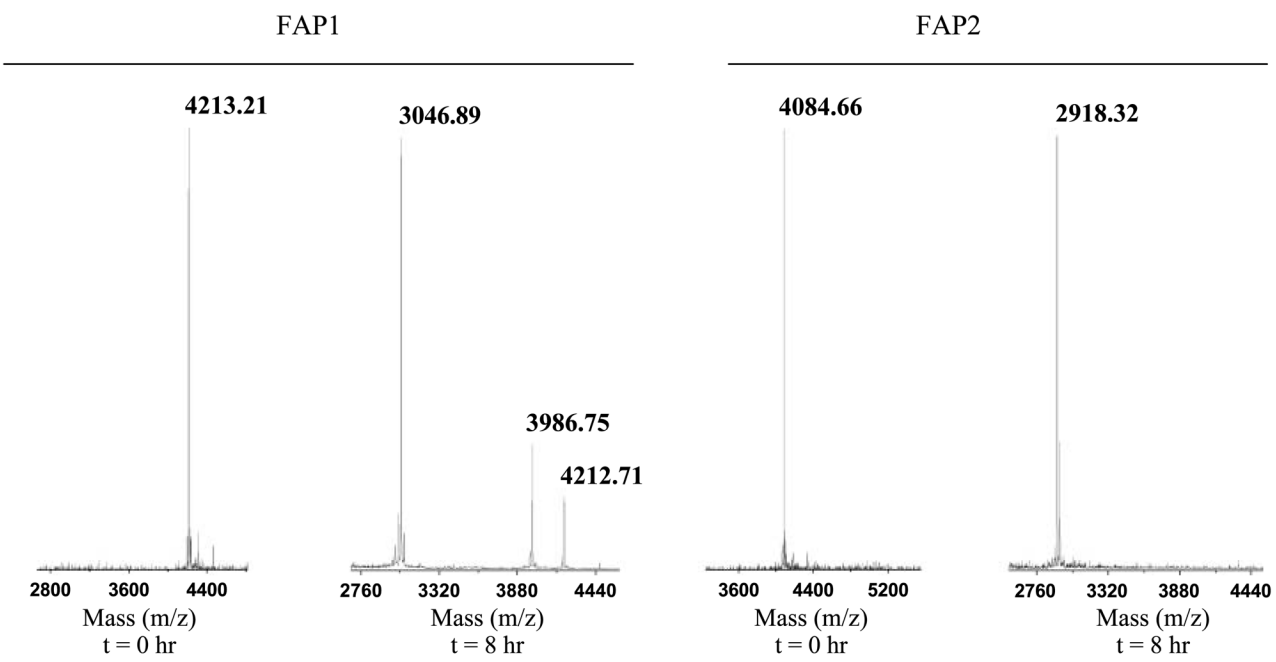

Figure 1.

FAP cleavage of the modified promelittin peptides. The prodomain sequence of modified protoxins (*FAP 1-5*) with cleavage site and mass of cleavage fragment delineated. MALDI-TOF analysis was used to evaluate the extent of cleavage. The relative intensity of each mass fragment is based on a comparison of the relative peak height for each individual trace, with the largest peak for each experiment arbitrarily set to 100. *Bottom,* representative MALDI trace for FAP1 and FAP2 (100 μg) at time 0 and 8 h after exposure to active FAP (2 μg total).

NIH-PA Author Manuscript

NIH-PA Author Manuscript

NIH-PA Author Manuscript

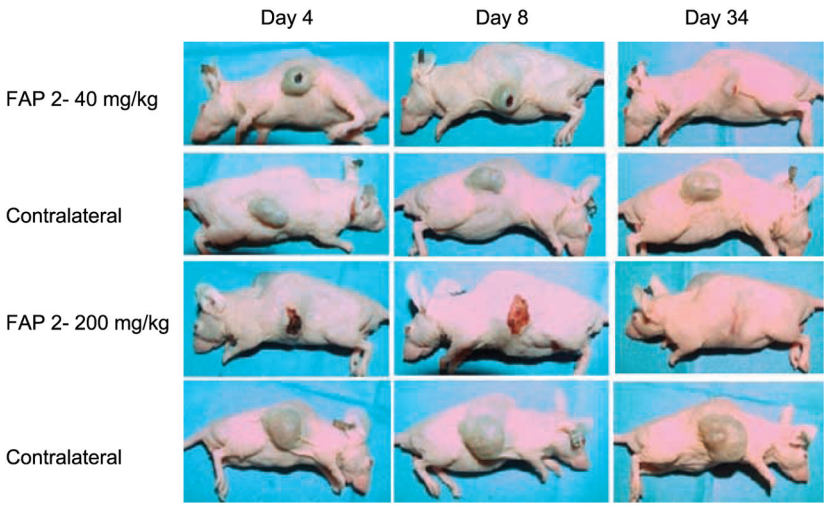

Figure 2.

Nude mice bearing LNCaP human prostate cancer xenografts on both flanks were treated with single intratumoral dose of FAP2 at the indicated concentration of FAP2 into the tumor in one flank, with saline injected into the tumor on the contralateral flank. Representative tumor response is shown for 1 animal at each dose level over a 34-d period.

NIH-PA Author Manuscript
NIH-PA Author Manuscript
NIH-PA Author Manuscript

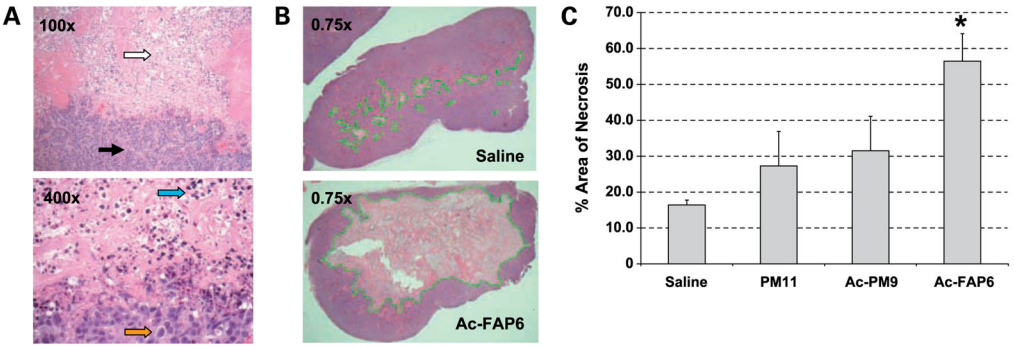

Figure 3.

Comparison of the effect of promelittin toxins on the viability of human MCF-7 breast cancer xenografts. **A,** H&E-stained tissue from xenograft treated with Ac-FAP6 shows unaffected tumor adjacent to the necrotic area at ×100 and ×400 magnification. *Top, white arrow,* area of necrotic tissue; *black arrow,* strand of stroma within the background of tumor cells. *Bottom, blue arrow,* pyknotic nuclei consistent with necrotic death; *orange arrow,* nuclei from a viable cell unaffected by toxin; **B,** evaluation of the extent of necrosis produced by the intratumoral injection of Ac-FAP6 at 96 h postinjection. H&E-stained cross-section of representative tumor treated with either Ac-FAP6 (45 mg/kg) or saline shows increased areas of necrosis (*pale pink area outlined in green*) in a background of viable tumor (*reddish purple*). Representative images shown at ×0.75 magnification; **C,** image analysis used to the determine the % area of necrosis calculated as the ratio of the cross-sectional area of nonviable tumor to area of total tumor for tumors treated intratumorally with single dose of 250 nmoles of indicated toxin or normal saline (*, $P <$ 0.05 by Student's *t* test for Ac-FAP6 versus saline control).

NIH-PA Author Manuscript
NIH-PA Author Manuscript
NIH-PA Author Manuscript

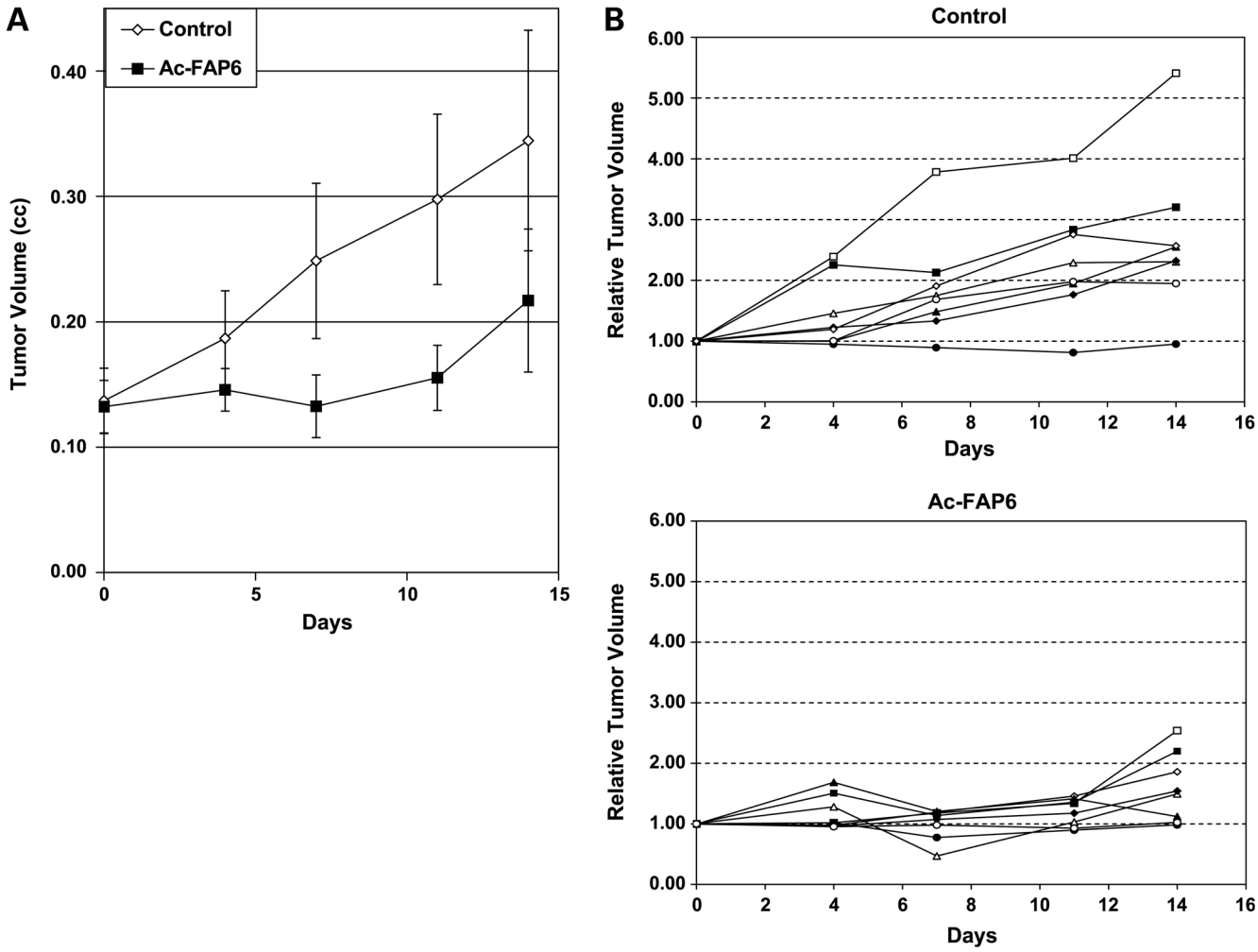

Figure 4.

Antitumor effect of a single intratumoral dose of Ac-FAP6 against MCF-7 human breast cancer xenografts. **A,** average tumor volume of saline control versus Ac-FAP6 (45 mg/kg) over a 14-d period ($n = 8$ mice per group; $P < 0.05$ for days 4, 7, and 11 by ANOVA); **B,** growth of individual saline-treated control tumors to Ac-FAP6–treated tumors over a 14-d period. Each trace represents the growth of an individual MCF-7 xenograft in each mouse.

NIH-PA Author Manuscript
NIH-PA Author Manuscript
NIH-PA Author Manuscript

Table 1

Prodomain amino acid sequence of promelittin peptides

Toxin		HD_{50} (μmol/L)	Net charge
PM11	APEPEPAPEPEAEADAEADPEA	>100	−3
PM11a	PEPEPAPEPEAEADAEADPEA	>100	−3
PM10	EPEPAPEPEAEADAEADPEA	>100	−3
PM10a	PEPAPEPEAEADAEADPEA	>100	−2
PM9	EPAPEPEAEADAEADPEA	95.5 ± 3.4	−2
PM9a	PAPEPEAEADAEADPEA	73.0 ± 4.7	−1
PM8	APEPEAEADAEADPEA	64.0 ± 4.2	−1
PM8a	PEPEAEADAEADPEA	59.3 ± 2.7	−1
PM7	EPEAEADAEADPEA	66.6 ± 2.9	−1
PM7a	PEAEADAEADPEA	52.0 ± 2.3	0
PM6	EAEADAEADPEA	55.9 ± 3.5	0
PM6a	AEADAEADPEA	48.4 ± 1.9	1
PM5	EADAEADPEA	37.6 ± 2.5	1
PM5a	ADAEADPEA	29.2 ± 1.8	2
PM4	DAEADPEA	22.3 ± 1.1	2
PM4a	AEADPEA	11.8 ± 0.6	3
PM3	EADPEA	8.6 ± 0.3	3
PM3a	ADPEA	6.2 ± 0.2	4
PM2	DPEA	4.7 ± 0.3	4
PM2a	PEA	1.8 ± 0.1	5
PM1	EA	1.7 ± 0.1	5
PM1a	A	1.5 ± 0.1	6
PM0		1.3 ± 0.1	6

NOTE: HD_{50}, concentration required to lyse 50% of RBC in a 2% RBC solution. Charge, net charge on the full length peptide.

NIH-PA Author Manuscript

NIH-PA Author Manuscript

NIH-PA Author Manuscript

Table 2

HD_{50} values and cytotoxicity of FAP Melittin protoxins against FAP-negative and FAP-positive MCF-7 human breast cancer cells

Toxin	HD_{50} (μmol/L)	IC_{50} (μmol/L)		
		FAP neg	FAP pos	Fold diff
FAP1	56.9 ± 3.1	45.6 ± 5.6	26.8 ± 1.1	1.7
FAP2	54.2 ± 2.2	35.1 ± 2.0	5.2 ± 0.4	6.7
FAP3	60.0 ± 3.7	33.1 ± 2.3	18.9 ± 1.7	1.8
FAP4	70.5 ± 5.1	50.1 ± 4.9	28.1 ± 2.2	1.8
FAP5	67.5 ± 3.5	27.6 ± 1.2	18.3 ± 2.0	1.5
Ac-FAP6	72.2 ± 3.6	47.9 ± 2.9	6.1 ± 0.3	7.9
Melittin	1.3 ± 0.1	1.4 ± 0.1	1.3 ± 0.2	1.1

Abbreviations: FAP neg, FAP negtive; FAP pos, FAP positive; fold diff, fold difference.